JOURNAL OF ENZYME INHIBITION AND MEDICINAL CHEMISTRY
2026, VOL. 41, NO. 1, 2755636
https://doi.org/10.1080/14756366.2026.2755636

Taylor & Francis
by informa

RESEARCH ARTICLE

OPEN ACCESS Check for updates

# Tramadol potentiates chemotherapy efficacy in hepatocellular carcinoma cells

Hsiu-Lung Fan[a], Shu-Ting Liu[b], Zih-Syuan Wu[b], Yi-Hsuan Huang[c], Shih-Ming Huang[b], Teng-Wei Chen[a] and Zhi-Fu Wu[c,d,e,f]

[a]Division of General Surgery, Department of Surgery, School of Medicine, College of Medicine, Tri-Service General Hospital, National Defense Medical University, Taipei City, Republic of China; [b]Graduate Institute of Biochemistry, College of Biomedical Sciences, National Defense Medical University, Taipei City, Republic of China; [c]Department of Anesthesiology, School of Medicine, College of Medicine, Tri-Service General Hospital, National Defense Medical University, Taipei City, Republic of China; [d]Department of Anesthesiology, E-Da Hospital, I-Shou University, Kaohsiung City, Taiwan, Republic of China; [e]Department of Anesthesiology, Faculty of Medicine, College of Medicine, Kaohsiung Medical University, Kaohsiung City, Taiwan, Republic of China; [f]Center for Regional Anesthesia and Pain Medicine, Wan Fang Hospital, Taipei Medical University, Taipei City, Taiwan, Republic of China

**ABSTRACT**

Hepatocellular carcinoma (HCC) is the sixth most common cancer and the third leading cause of cancer-related deaths, leading to poor responses to chemotherapy. Cancer-related pain affects up to 90% of these patients, significantly impairing their quality of life. Tramadol, a prescribed analgesic for cancer pain, has shown anti-tumour effects in various malignancies, yet its potential in HCC remains largely unexplored. In this study, we investigated tramadol's anti-proliferative, pro-apoptotic, and autophagy-inducing effects in HepG2, Hep3B, and Huh7 cell lines. Tramadol significantly inhibits cell proliferation in a dose-dependent manner, leading to a reduction in the S-phase and subG1 phase accumulation. It induces apoptosis in HepG2 and Hep3B, increases late apoptosis/necrosis, and enhances autophagy. Additionally, tramadol increased the cytotoxicity of cisplatin and 5-fluorouracil, with significant reductions in their IC50 values. Overall, tramadol inhibits HCC growth, promotes apoptosis, and enhances chemotherapy efficacy, suggesting it could be a dual-benefit therapeutic strategy for HCC.

**ARTICLE HISTORY**
Received 6 July 2026
Revised 12 October 2026
Accepted 22 October 2026

**KEYWORDS**
Tramadol; hepatocellular carcinoma; apoptosis; combinatory therapy

## Introduction

Hepatocellular carcinoma (HCC) is the sixth most diagnosed malignancy and the third leading cause of cancer-related mortality worldwide, highlighting its significant impact on global health.[1] The burden of HCC has risen dramatically in recent decades. The Global Burden of Disease Study reported over 529,000 new cases and 483,000 deaths in 2021, reflecting more than a 50% increase in both incidence and mortality compared to twenty years ago.[2] Similarly, estimates from the World Health Organisation indicated that liver cancer accounted for over 900,000 new cases and 800,000 deaths in 2020, with annual mortality rates projected to approach one million by 2030.[3] These alarming epidemiological trends underscore the urgent need for more effective prevention and treatment strategies.

HCC accounts for approximately 90% of primary liver cancers and typically develops in the context of chronic hepatitis B virus (HBV) or hepatitis C virus (HCV) infections, aflatoxin exposure, and metabolic disorders.[4] The insidious onset and absence of specific symptoms during the early stages contribute to delayed diagnoses, with most patients presenting at advanced, often incurable, stages. The relative 5-year survival rate for patients with HCC is a mere 18%.[5] Curative interventions, such as hepatic resection and liver transplantation, are generally limited to those diagnosed at an early stage. For patients who are not suitable candidates

**CONTACT** Teng-Wei Chen doc20264@gmail.com Division of General Surgery, Department of Surgery, School of Medicine, College of Medicine; Tri-Service General Hospital, National Defense Medical University, Taipei City114, Republic of China; Zhi-Fu Wu aneswu@gmail.com Department of Anesthesiology, School of Medicine, College of Medicine; Tri-Service General Hospital, National Defense Medical University, Taipei City114, Republic of China.

© 2026 The Author(s). Published by Informa UK Limited, trading as Taylor & Francis Group.
This is an Open Access article distributed under the terms of the Creative Commons Attribution License (http://creativecommons.org/licenses/by/4.0/), which permits unrestricted use, distribution, and reproduction in any medium, provided the original work is properly cited. The terms on which this article has been published allow the posting of the Accepted Manuscript in a repository by the author(s) or with their consent.

for surgery, radiofrequency ablation serves as the primary local treatment for early lesions, while transarterial chemoembolization (TACE) is typically utilised for intermediate-stage disease. Systemic therapies are generally reserved for advanced-stage HCC.[6] Additionally, HCC is intrinsically resistant to many anticancer agents, resulting in poor responsiveness to conventional chemotherapy among affected patients.

Among chemotherapeutic agents, 5-fluorouracil (5-FU) and cisplatin are the most commonly used in clinical practice for treating HCC patients. 5-FU, a heterocyclic aromatic antimetabolite, inhibits thymidylate synthase, thereby blocking thymidine synthesis, disrupting DNA replication, and ultimately inhibiting tumour cell proliferation.[7] However, the emergence of acquired resistance to 5-FU during treatment is frequently observed, significantly limiting its long-term efficacy. Cisplatin, the first metal-based anticancer agent developed for HCC, exerts its cytotoxic effect by interfering with DNA repair mechanisms, inducing DNA damage, and triggering apoptosis.[8] Nonetheless, prolonged use of cisplatin is associated with cumulative toxicities, including nephrotoxicity and ototoxicity.[9] Despite its established role in treating other malignancies, conventional chemotherapy offers only modest benefits in HCC, emphasising the urgent need for novel and more effective therapeutic strategies to enhance patient outcomes.

Up to 90% of patients with HCC experience cancer-related pain, primarily resulting from tumour overgrowth, invasion or infiltration of surrounding tissues, and stimulation of nociceptors in adjacent organs.[10] Typically, this pain ranges from moderate to severe and persists throughout the course of the disease. Unrelieved pain significantly diminishes quality of life, contributes to functional decline, and may even accelerate disease progression by exacerbating systemic stress responses. Additionally, chronic pain imposes substantial psychological distress and financial burdens on patients and their families, highlighting the urgent need for effective pain management strategies as a crucial component of HCC care. Opioids are widely used for pain management in cancer patients, including those with HCC.[11] The three subtypes of opioid receptors—μ, κ, and δ—are involved in cancer progression and can influence long-term patient outcomes. Specifically, the μ-opioid receptor has been shown to promote tumour initiation and serves as a molecular marker for poor prognosis in HCC.[12–14] Research indicates that downregulation of the κ-opioid receptor is associated with unfavourable outcomes in HCC patients, while upregulation of the δ-opioid receptor has been linked to the progression of human breast cancer.[15,16] Conversely, morphine has been found to suppress lung cancer cell proliferation through its interaction with the opioid growth factor receptor.[17] Furthermore, future studies exploring the effects of opioids on non-opioid receptors may enhance our understanding of the role of opioids in cancer biology.

Tramadol is a widely prescribed analgesic for managing both acute and chronic pain, with its analgesic activity stemming from two primary mechanisms: agonism at μ-opioid receptors and the inhibition of neuronal reuptake of norepinephrine and serotonin.[18] In addition to its pain-relieving properties, emerging evidence suggests that tramadol may also possess anti-cancer effects. Retrospective clinical studies have indicated that tramadol use is associated with reduced postoperative recurrence and mortality in patients with breast cancer.[19] Preclinical models demonstrate that clinically relevant doses of tramadol can suppress breast cancer cell proliferation in orthotopic mouse models.[20] Similarly, studies on human endometrial carcinoma cells have shown that tramadol inhibits cell growth, induces apoptosis, enhances reactive oxygen species (ROS) production, and promotes mitochondrial dysfunction.[21] Furthermore, tramadol has been found to synergistically enhance the cytotoxic effects of doxorubicin in triple-negative breast cancer cells.[22] Despite these promising findings, it remains unclear whether tramadol exerts similar anti-tumour effects in HCC, highlighting the need for systematic investigation in this area.

Therefore, we undertook this study to assess the anti-proliferative effects of tramadol in HCC cell lines, including HepG2, Hep3B, and Huh7 cells, and to investigate its potential mechanisms as a chemosensitizer for cisplatin and 5-FU. Our findings underscore tramadol's potential as a dual-function agent, offering both analgesic relief and direct anti-cancer activity in HCC.

## Methods and materials

### *Cell culture and reagents*

HepG2, Hep3B, and Huh7 HCC cell lines were obtained from the American Type Culture Collection (ATCC; Manassas, VA, USA). The cells were cultured in Dulbecco's Modified Eagle Medium (DMEM) supplemented

with 10% foetal bovine serum (FBS) and 1% penicillin/streptomycin solution (Invitrogen, Waltham, MA, USA). Tramadol, cisplatin, 5-FU, thiazolyl blue tetrazolium bromide (MTT), propidium iodide (PI), and acridine orange (AO) (Cat. No. A8097) were purchased from Sigma Aldrich (St. Louis, MO, USA).

### *Cellular proliferation BrdU assay*

HCC cells ($5\times10^5$ per well) were plated in 6-well plates and incubated overnight. For the cell proliferation assays, the cells were treated with tramadol at various concentrations (0, 0.2, 0.4, 0.6, 0.8, and 1 mg/mL) for 24 h, followed by a 1-h incubation with 10 µM BrdU using the BrdU Flow Kit (BD Pharmingen, San Diego, CA, USA). After labelling, the culture medium was removed, and the cells were fixed at room temperature for 30 min. The fixed cells were then stained with a FITC-conjugated anti-BrdU antibody according to the manufacturer's instructions. After washing, the cells were counterstained with 7-AAD and analysed using a BD FACSCalibur™ flow cytometer. Data acquisition and analysis were conducted with CellQuest Pro software (version 5.1) from BD Biosciences (Franklin Lakes, NJ, USA).

### *Cell cycle profiles analysis*

HCC cells ($5\times10^5$ per well) were plated in 6-well plates and incubated overnight. The following day, the cells were treated with tramadol at concentrations of 0, 0.2, 0.4, 0.6, 0.8, and 1 mg/mL for 24 h. After treatment, the cells were fixed in 70% ice-cold ethanol and stored at −20 °C overnight. The fixed cells were then centrifuged at 1,000 rpm for 5 min, washed twice with ice-cold PBS containing 1% FBS, and stained with a PI solution (5 µg/mL PI, 0.5% Triton X-100, and 0.5 µg/mL RNase A in PBS) for 30 min at 37 °C in the dark. A total of 10,000 events per sample were acquired using a BD FACSCalibur™ flow cytometer, and the data were analysed with CellQuest Pro software.

### *Cell viability and combination index analysis*

HCC cells ($5\times10^3$ per well) were plated in 96-well plates and allowed to incubate overnight. The next day, the cells were treated with tramadol at concentrations ranging from 0 to 1 mg/mL (0, 0.2, 0.4, 0.6, 0.8, and 1) for 24 h. Cell viability was evaluated using the MTT assay. Specifically, 0.5 mg/mL MTT solution, prepared in phosphate-buffered saline (PBS), was added to each well and incubated for 4 h at 37 °C. After incubation, the supernatant was removed, and 100 µL of dimethyl sulfoxide (DMSO) was added to dissolve the formazan crystals. Absorbance was measured at 570 nm with a background correction at 650 nm using a Varioskan LUX microplate reader (Thermo Fisher Scientific, Vantaa, Finland). Relative cell viability was expressed as a percentage of the vehicle control, which was set at 100%. For drug combination experiments, the combination index (CI) was calculated using CalcuSyn software (version 2) (Biosoft, Cambridge, UK) to generate isobolograms, where a CI < 1 indicates synergy and a CI > 1 suggests antagonism.[23]

### *Apoptosis analysis*

HCC cells ($5\times10^5$ per well) were plated in 6-well plates and allowed to incubate overnight. The following day, the cells were treated with tramadol at varying concentrations (0, 0.2, 0.4, 0.6, 0.8, and 1 mg/mL) for a duration of 24 h. After treatment, the cells were washed twice with ice-cold PBS and resuspended in 200 µL of binding buffer. To assess apoptosis, 5 µL of Annexin V-PE and 10 µL of 7-AAD (5 µg/mL) were added to the samples, which were then incubated for 15 min at room temperature in the dark. The percentage of apoptotic cells was determined using a BD FACSCalibur™ flow cytometer, with data analysed through CellQuest Pro software.

### *Mitochondrial membrane potential analysis*

HCC cells ($5\times10^5$ per well) were plated in 6-well plates and allowed to incubate overnight. The next day, fresh medium containing tramadol at concentrations of 0, 0.2, 0.4, 0.6, 0.8, and 1 mg/mL was added, and the cells were incubated for 24 h. After the incubation, both adherent and suspended cells were collected, washed once with PBS, and then treated with JC-1 working solution diluted in 1× binding buffer for 30 min at 37 °C in the dark. Following the staining process, cells were washed twice with PBS,

resuspended in 500 µL of 1× binding buffer, and analysed for fluorescence using a BD FACSCalibur™ flow cytometer with CellQuest Pro software. The mitochondrial membrane potential (ΔΨm) was evaluated by calculating the ratio of red (aggregates) to green (monomers) fluorescence intensity, with a lower red/green ratio indicating mitochondrial depolarisation.

### *Western blot*

HCC cells ($5\times10^5$/well) were seeded into 6-well plates overnight. The following day, fresh medium containing tramadol (0, 0.2, 0.4, 0.6, 0.8, and 1 mg/mL) was added, and cells were incubated for 24 h. After tramadol treatment, cells were lysed in radioimmunoprecipitation assay buffer supplemented with protease and phosphatase inhibitors to extract total protein. Protein concentrations were determined using a DC Protein Assay Kit (Bio-Rad, Hercules, CA, USA), and equal amounts of protein (30 µg per lane) were separated by SDS–PAGE and transferred onto polyvinylidene difluoride (PVDF) membranes (Millipore, Bedford, MA, USA). PVDF membranes were blocked with 5% non-fat dry milk in TBST (20 mM Tris-HCl, 150 mM NaCl, 0.1% Tween-20, pH 7.4) for 1 h at room temperature and then incubated with primary antibodies overnight at 4 °C. After TBST washing, membranes were incubated with HRP-conjugated secondary antibodies for 1 h at room temperature. Primary antibodies against α-actinin (ACTN, H-2, sc-17829), p53 (DO-1, sc-125), PCNA (F-2, sc-25280), FASN (A-5, sc-55580), p62 (D-3, sc-28359), and Bax (2D2, sc-20067) were purchased from Santa Cruz Biotechnology (Santa Cruz, CA, USA), and primary antibodies against CHOP (L63F7, 2895), LC3B (2775), PARP (19F4, 9546), Beclin-1 (D40C5, 3495), EGFR (D38B1, 4267), H3 (9715), p-eIF2α (Ser51, 9721), e-IF2α (9772), ATF4 (11815), HIF1α (14179), and Caspase-3 (9662) were obtained from Cell Signalling Technology (Danvers, MA, USA), and primary antibodies against Cyclin D1 (EPR2241, ab134175), and p21 (EPR362, ab109520) were purchased from Abcam (Cambridge, UK). xCT (ARG57998) and GPX4 (ARG41400) primary antibodies were purchased from Arigo biolaboratories. Thereafter, the blots were incubated with KPL peroxidase-labeled antibodies (anti-mouse IgG, 5220–0341, 074–1806; and anti-rabbit IgG, 5220–0336, 074–1506, Seracare). The immunoreactive proteins were detected using ECL™ Western Blotting Detection Reagent and Amersham Hyperfilm™ ECL (GE Healthcare, USA). The prestained protein ladder (Prep1025G) was purchased from Bioman Scientific Co., LTD (New Taipei, Taiwan).

### *Autophagy acridine orange (AO) staining*

HCC cells ($5\times10^5$ per well) were plated in 6-well plates and allowed to incubate overnight. The next day, fresh medium containing various concentrations of tramadol (0, 0.2, 0.4, 0.6, 0.8, and 1 mg/mL) was added, and the cells were incubated for 24 h. After tramadol treatment, the HCC cells were stained with 1 µg/mL AO for 30 min at 37 °C in the dark. The cells were then washed three times with PBS to remove any excess dye, resuspended in fresh PBS, and immediately analysed for fluorescence intensity using a BD FACSCalibur™ flow cytometer with CellQuest Pro software.

***GSH/GSSG measurement.*** We utilised the GSH/GSSG-Glo™ Assay (Promega) to evaluate the GSH/GSSG ratio. In summary, HepG2 and Hep3B cells were plated at a density of $1.5\times10^4$ cells per well in a 96-well culture plate. The following day, cells were treated with either 0.6 mg/mL tramadol, 10 µM cisplatin, or 250 µM 5-FU for 24 h. After treatment, the cells were washed with PBS and then treated with 50 µL of total GSH lysis reagent for total GSH measurements or oxidised GSH lysis reagent for GSSG measurements. Next, 50 µL of Luciferin Generation Reagent was added to each well, mixed, and incubated for 30 min. Subsequently, 100 µL of Luciferin Detection Reagent was added, mixed well, and incubated for another 15 min before measuring luminescence. The GSH/GSSG ratio was calculated from the luminescence values expressed in relative light units (RLU) using the formula: (total GSH RLU – GSSG RLU)/(GSSG RLU/2).

### *Statistics*

The values are presented as means ± standard deviations (SD) from a minimum of three independent experiments. Comparisons between groups were performed using Student's t-tests, while analysis of variance (ANOVA) was used for comparisons among multiple groups, utilising SPSS 20.0 for Windows (SPSS, Chicago, IL). A $p$ values of less than 0.05 was considered statistically significant.

## Results

### *Tramadol inhibited cellular proliferation, altered the cell cycle profile, and disrupted mitochondrial membrane potential in HCC cells*

Direct quantification of DNA synthesis is a reliable method for assessing cell proliferation and is commonly employed in toxicity testing and cellular health monitoring. In this study, we investigated the effects of tramadol on the proliferative capacity of HCC cell lines, specifically HepG2, Hep3B, and Huh7. BrdU incorporation assays demonstrated that tramadol significantly inhibited cell proliferation in a dose-dependent manner across all three cell lines, with statistical significance indicated by $p$(ANOVA) = $3.1\times10^{-14}$ for HepG2, $p$(ANOVA) = $6.3\times10^{-16}$ for Hep3B, and $p$(ANOVA) = $4.9\times10^{-14}$ for Huh7 (Figure 1A). Given that BrdU is incorporated during the S phase, these results suggest potential effects on cell cycle progression. Further analysis using PI staining confirmed that tramadol significantly reduced the S phase population in all three cell lines in a dose-dependent manner ($p$(ANOVA) = $1.4\times10^{-13}$ for HepG2, $p$(ANOVA) = $6.2\times10^{-17}$ for Hep3B, and $p$(ANOVA) = $3.4\times10^{-14}$ for Huh7) while increasing the subG1 population in HepG2 and Hep3B cells ($p$(ANOVA) = $3.4\times10^{-5}$ and $p$(ANOVA) = $6.0\times10^{-11}$, respectively), with a less pronounced effect observed in Huh7 cells ($p$(ANOVA) = $4.5\times10^{-2}$) (Figure 1B). In the G1 phase, tramadol tended to increase the proportion of Huh7 cells in a dose-dependent manner ($p$(ANOVA) = $4.7\times10^{-15}$), whereas it increased the proportion of HepG2 and Hep3B cells at doses below 1 mg/mL ($p$(ANOVA) = $2.6\times10^{-10}$ for HepG2 and $p$(ANOVA) = $2.8\times10^{-9}$ for Hep3B). The G2/M population generally showed a decrease in the proportion of Huh7 cells in a dose-dependent manner ($p$(ANOVA) = $4.0\times10^{-5}$). In contrast, lower doses of tramadol reduced the proportion of the G2/M population in HepG2 and Hep3B cells; however, treatment with doses exceeding 0.8 mg/mL for HepG2 or 1 mg/mL for Hep3B resulted in an increase in the G2/M populations.

Loss of mitochondrial membrane potential (ΔΨm) is an early characteristic of apoptosis.[24] JC-1 staining, a widely utilised method for evaluating ΔΨm, distinguishes between red-fluorescent aggregates in healthy mitochondria and green-fluorescent monomers in depolarised mitochondria. Our results showed that tramadol significantly increased the population of JC-1 monomers in HepG2, Hep3B, and Huh7 cells, with the most pronounced loss of ΔΨm observed in HepG2 cells (Figure 2). The red-to-green fluorescence ratios were decreased across all three cell lines ($p$(ANOVA) = $1.4\times10^{-12}$ for HepG2, $p$(ANOVA) = $4.5\times10^{-9}$ for Hep3B, and $p$(ANOVA) = $3.4\times10^{-5}$ for Huh7), indicating mitochondrial depolarisation and further supporting tramadol's pro-apoptotic effect in HCC cells. Given these findings regarding the effects of tramadol on cellular proliferation, cell cycle distribution, and mitochondrial membrane potential in various HCC cell lines, we chose to focus on HepG2 and Hep3B cells to further investigate the potential impacts of tramadol on endoplasmic reticulum (ER) stress-mediated apoptosis and autophagy, as well as its effects in combination with chemotherapeutics, such as cisplatin and 5-FU.

### *Tramadol induced apoptosis and autophagy in HCC cells*

The subG1 phase indicates the presence of cells that have undergone apoptosis and is characterised by fragmented DNA and reduced DNA content compared to the G1 phase. Since tramadol increased the subG1 population in HepG2 and Hep3B cells—though not in Huh7 cells—in a dose-dependent manner, we further explored its effects on cytotoxicity and apoptosis specifically in HepG2 and Hep3B cells. Our findings revealed that tramadol suppressed cell viability in both cell lines, with IC50 values of 0.9 mg/mL for HepG2 cells and 1.2 mg/mL for Hep3B cells ($p$(ANOVA) = $1.3\times10^{-11}$ and $p$(ANOVA) = $8.7\times10^{-6}$) (Figure 3A). Additionally, tramadol significantly promoted late apoptosis and necrosis in HepG2 cells ($p$(ANOVA) = $2.0\times10^{-10}$ and $p$(ANOVA) = $4.3\times10^{-8}$) and both early and late apoptosis in Hep3B cells ($p$(ANOVA) = $2.1\times10^{-5}$ and $p$(ANOVA) = $4.7\times10^{-8}$) (Figure 3B). Interestingly, tramadol also decreased the population of early apoptotic cells in HepG2 cells ($p$(ANOVA) = $2.9\times10^{-5}$). To further elucidate the molecular mechanisms underlying tramadol-induced apoptosis, we assessed the expression of key apoptotic and stress-related proteins through Western blotting. Specifically, we analysed CHOP, a marker of ER stress-mediated apoptosis; cleaved poly(ADP-ribose) polymerase (cPARP), which indicates the execution phase of caspase-dependent apoptosis; and p53, a critical regulator of DNA damage-induced apoptotic pathways. HepG2 cells are characterised by the expression of wild-type p53, whereas Hep3B cells are completely devoid of p53 expression.[25] Accordingly, p53 protein levels were undetectable in Hep3B cells,

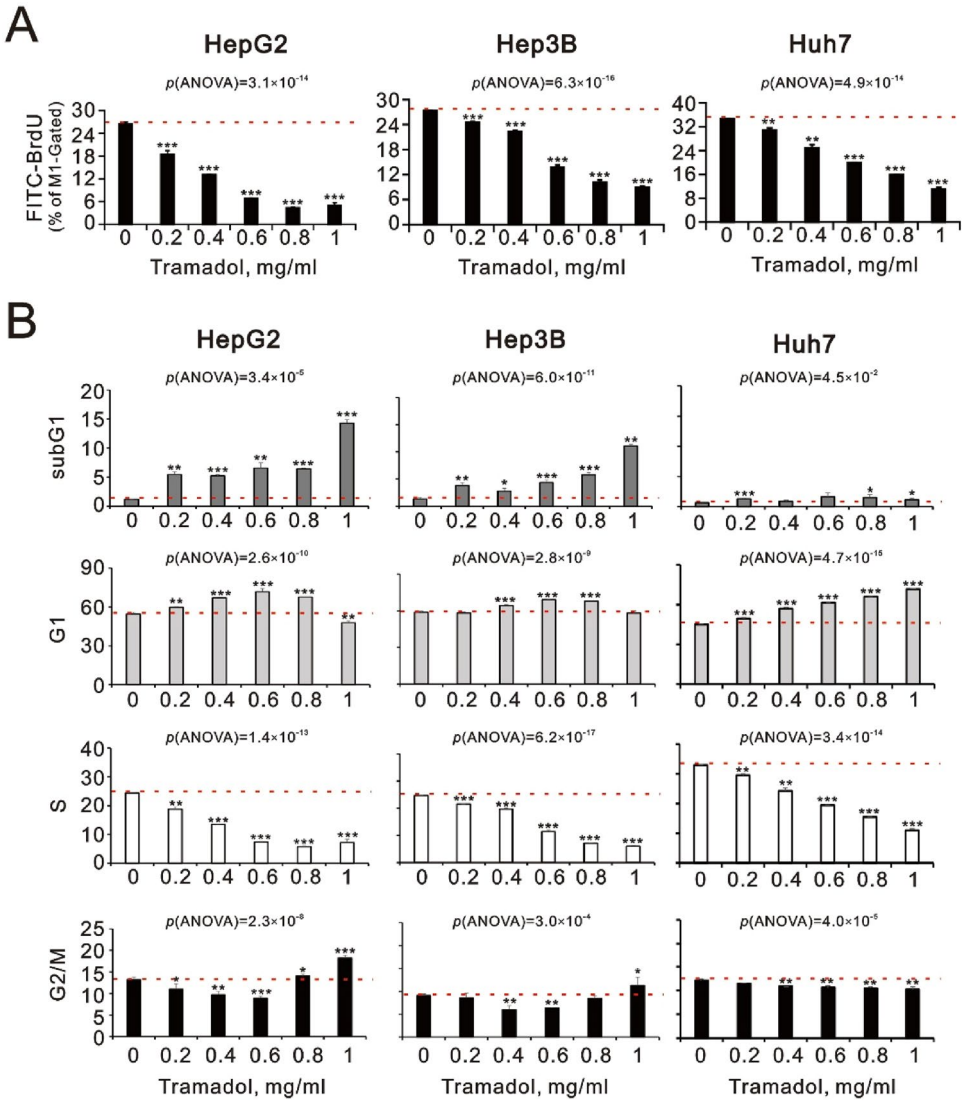



**Figure 1.** Effect of tramadol on cell proliferation and cell cycle profiles of human hepatocellular carcinoma cells. (**A**) HepG2, Hep3B, and Huh7 cells were treated with tramadol at concentrations of 0, 0.2, 0.4, 0.6, 0.8, and 1 mg/mL for 24 h, and cell proliferation was assessed by BrdU incorporation using flow cytometry. (**B**) HepG2, Hep3B, and Huh7 cells were treated with tramadol at concentrations of 0, 0.2, 0.4, 0.6, 0.8, and 1 mg/mL for 24 h, and cell cycle profiles were assessed by PI staining using flow cytometry. (**A and B**) The dashed red line is the level for the vehicle control. Bars depict the means ± SDs of three independent experiments. Statistical analysis was performed using one-way ANOVA with Tukey's multiple comparisons (**$p < 0.01$, ***$p < 0.001$ vs. untreated control).

while tramadol treatment resulted in a dose-dependent reduction of p53 levels in HepG2 cells (Figure 3C). Furthermore, tramadol elevated the expression of C/EBP homologous protein (CHOP) in both HepG2 and Hep3B cells. The transcription factors ATF4 and hypoxia-inducible factor 1 alpha (HIF1α) are both known to regulate *CHOP* mRNA expression.[26,27] Notably, tramadol has been shown to enhance HIF1α protein stability in breast cancer cells.[28] In HepG2 and Hep3B cells, tramadol induced ATF4 expression in a dose-dependent manner, while HIF1α was not similarly affected. Regarding apoptotic markers, cleaved PARP (cPARP) and cleaved Caspase-3 (cCaspase-3) were observed in HepG2 cells at a tramadol concentration of 1 mg/mL. In Hep3B cells, cPARP became detectable starting at 0.6 mg/mL, while cCaspase-3 was detected from 0.8 mg/mL, with both markers increasing in a dose-dependent manner. Bax, a key regulator of the intrinsic apoptosis pathway, is directly regulated by p53.[29] Our findings demonstrate that tramadol suppresses Bax expression in a dose-dependent manner in both HepG2 and Hep3B cells (Figure 3C).

Given that tramadol induced mitochondrial depolarisation and apoptosis in HCC cells, we next investigated whether it also modulates autophagy. Considering that mitochondrial damage can

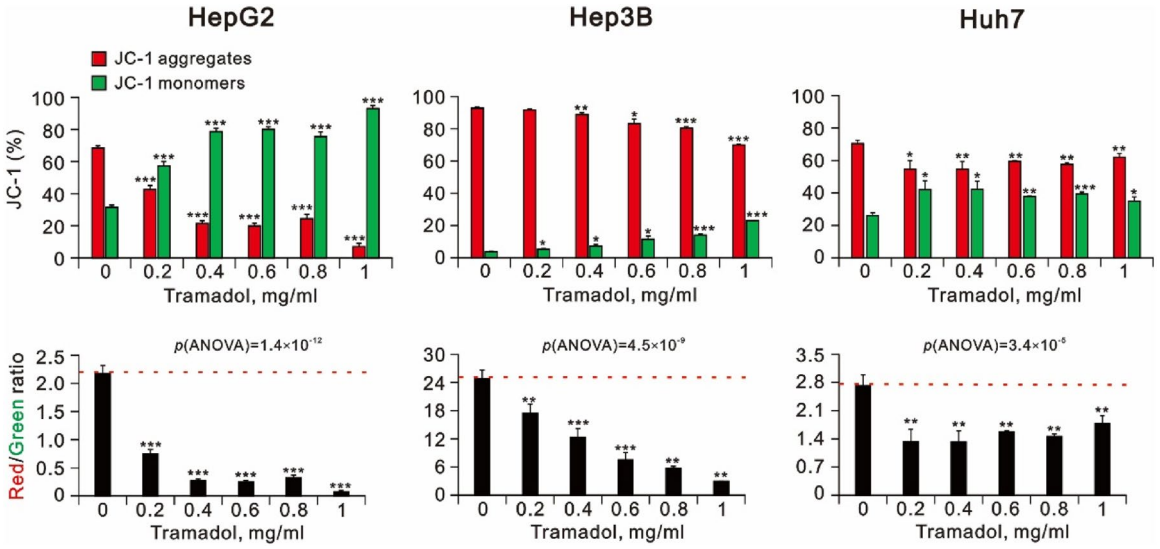



**Figure 2.** Effects of tramadol on mitochondrial membrane potential in human hepatocellular carcinoma cells. HepG2 and Hep3B cells were treated with tramadol at 0, 0.2, 0.4, 0.6, 0.8, and 1 mg/mL for 24 h, and mitochondrial membrane potential was evaluated by JC-1 staining using flow cytometry. The dashed red line is the level for the vehicle control. Bars depict the means ± SDs of three independent experiments. Statistical analysis was performed using one-way ANOVA with Tukey's multiple comparisons (*$p < 0.05$, **$p < 0.01$, ***$p < 0.001$ vs. untreated control).

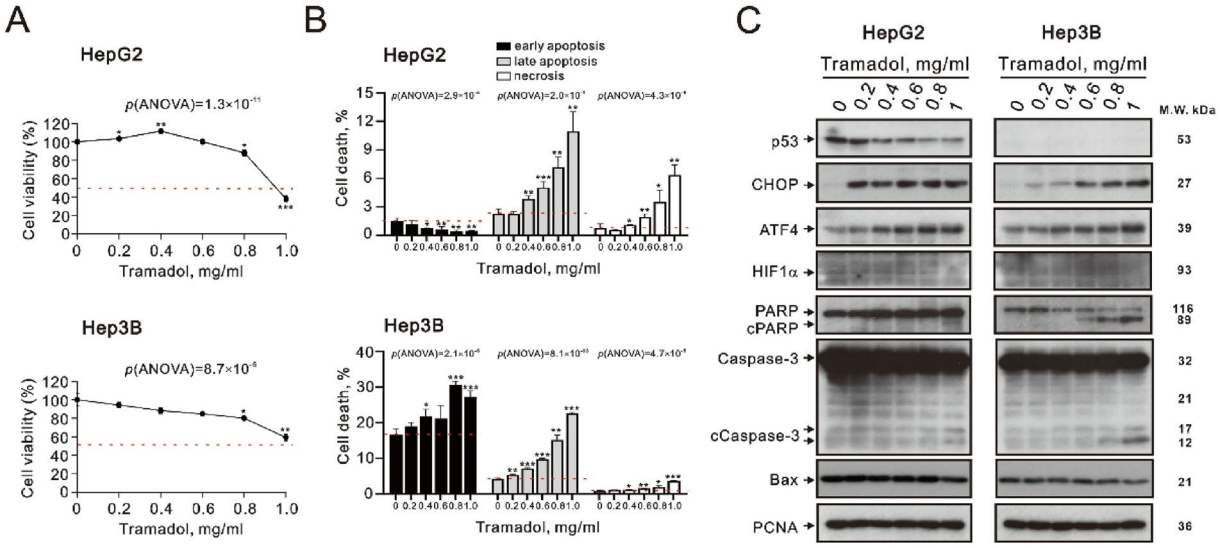



**Figure 3.** Effects of tramadol on cell viability and apoptosis in human hepatocellular carcinoma cells. (**A**) HepG2 and Hep3B cells were treated with tramadol at concentrations of 0, 0.2, 0.4, 0.6, 0.8, and 1 mg/mL for 24 h. Cell viability measured using the MTT method. (**B**) HepG2 and Hep3B cells were treated with tramadol at 0, 0.2, 0.4, 0.6, 0.8, and 1 mg/mL for 24 h, and apoptosis was evaluated by PE–Annexin V/7-AAD staining using flow cytometry. (**A and B**) The dashed red line is the level for the vehicle control. Bars depict the means ± SDs of three independent experiments. Statistical analysis was performed using one-way ANOVA with Tukey's multiple comparisons (*$p < 0.05$, **$p < 0.01$, ***$p < 0.001$ vs. untreated control). (**C**) HepG2 and Hep3B cells were treated with tramadol at 0, 0.2, 0.4, 0.6, 0.8, and 1 mg/mL for 24 h. The cell lysates, containing 30 µg of total protein, were analysed by Western blotting using antibodies targeting p53, CHOP, ATF4, HIF1α, cPARP, Caspase-3, and Bax. PCNA served as the loading control for protein levels.

trigger mitophagy, we hypothesised that tramadol might regulate autophagy, potentially contributing to its pro-apoptotic effect. To assess autophagy, we performed acridine orange (AO) staining, which selectively labels acidic vesicular organelles (AVOs), a hallmark of autophagic activity. The results indicated that tramadol significantly increased autophagy in both HepG2 and Hep3B cells in a dose-dependent manner ($p$(ANOVA) = $1.7 \times 10^{-12}$ and $p$(ANOVA) = $4.8 \times 10^{-10}$) (Figure 4A). To further

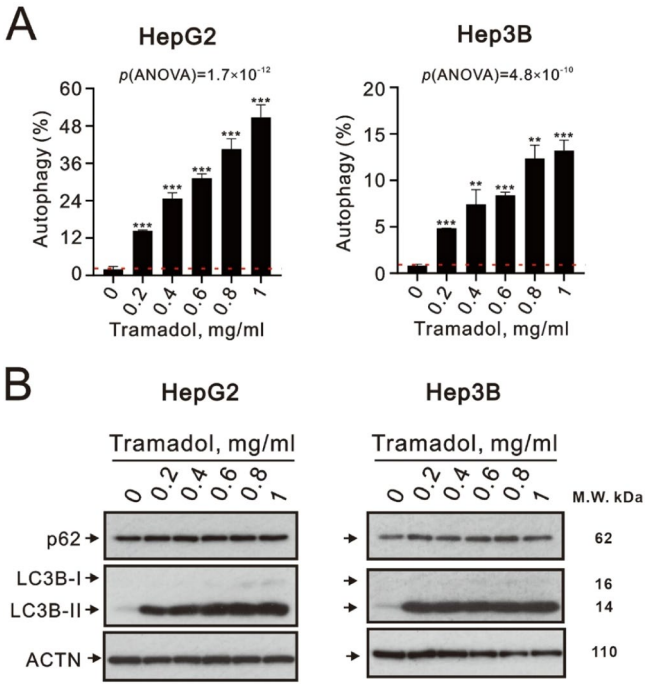



**Figure 4.** Effects of tramadol on autophagy in human hepatocellular carcinoma cells. (**A**) HepG2 and Hep3B cells were treated with tramadol at 0, 0.2, 0.4, 0.6, 0.8, and 1 mg/mL for 24 h, stained with AO, and autophagy was assessed and quantified by flow cytometry. The dashed red line is the level for the vehicle control. Bars depict the means ± SDs of three independent experiments. Statistical analysis was performed using one-way ANOVA with Tukey's multiple comparisons (**$p < 0.01$, ***$p < 0.001$ vs. untreated control). (**B**) HepG2 and Hep3B cells were treated with tramadol at 0, 0.2, 0.4, 0.6, 0.8, and 1 mg/mL for 24 h. The cell lysates, containing 30 µg of total protein, were analysed by Western blotting using antibodies targeting p62 and LC3B. ACTN was used as a loading control.

confirm these findings, we evaluated the expression of key autophagy markers, LC3B-II (microtubule-associated protein 1 light chain 3 beta-II) and p62, by Western blotting. LC3B is crucial for autophagosome formation, and its conversion from LC3B-I to LC3B-II is widely accepted as a marker of autophagy. Meanwhile, p62 (also known as SQSTM1) serves as a selective substrate for autophagy, and its degradation reflects ongoing autophagic processes.[30] Western blot analysis revealed a dose-dependent increase in LC3B-II levels in both cell lines, indicating enhanced the percentage of autophagy induced by tramadol (Figure 4B). Additionally, tramadol treatment resulted in increased levels of p62 in both cell lines.

### *Tramadol exhibited a synergistic effect with cisplatin or 5-FU in HCC cells*

To explore the potential of tramadol to enhance conventional chemotherapy, we assessed its combinatorial effects with commonly used HCC chemotherapeutic agents, cisplatin and 5-FU. HCC cells were co-treated with tramadol and each chemotherapeutic agent at varying concentrations, and cell viability was measured. Combination index (CI) analysis, calculated using the Chou–Talalay method, was performed to quantitatively evaluate drug interactions.[23] A CI value of less than 1 indicates synergism, a value of 1 suggests an additive effect, and a value greater than 1 indicates antagonism. The results demonstrated that tramadol significantly enhanced the cytotoxic effects of both cisplatin and 5-FU in a synergistic manner (CI < 1) across both cell lines (Figure 5). This suggests that tramadol may enable dose reduction of chemotherapeutics while preserving or even enhancing their anticancer efficacy. Notably, in HepG2 cells, co-treatment with tramadol reduced the IC50 of cisplatin from 58 µM to 0.7 µM and that of 5-FU from 2710 µM to 8.4 µM (Figure 5A and B), indicating a remarkable dose-sparing effect and improved chemotherapeutic efficacy. Similarly, tramadol lowered the IC50 of cisplatin from 32 µM to 2.6 µM and in Hep3B cells (Figure 5C). 5-FU monotherapy failed to reach 50% inhibition in Hep3B cells within the tested concentration range (IC50 > 800 µM). In contrast, combination treatment dramatically enhanced cell killing, lowering the effective IC50 to 10.7 µM (Figure 5D).

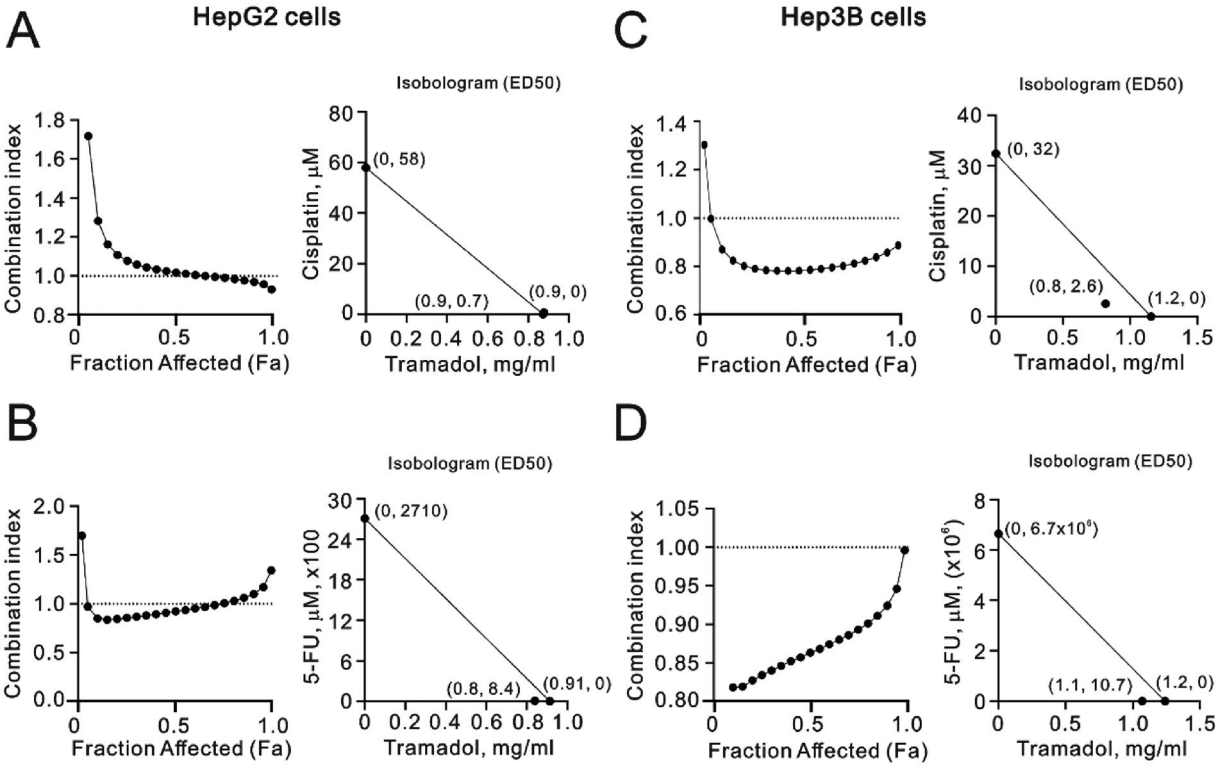



**Figure 5.** Combination indexes for tramadol with cisplatin or 5-FU in human hepatocellular carcinoma cells. (**A and B**) HepG2 and (**C and D**) Hep3B cells were treated with tramadol at 0, 0.2, 0.4, 0.6, 0.8, 1, 1.5, and 2 mg/mL combined with (**A and C**) 0, 0.156, 0.3125, 0.625, 1.25, 2.5, 5, 10, 20, and 40 µM cisplatin or (**B and D**) 0, 10, 20, 50, 100, 200, 250, 350, 500, and 800 µM 5-FU for 24 h. Cell viability was measured using the MTT method. Isobolograms (ED50) were calculated using CalcuSyn software.

### *Tramadol combined with cisplatin or 5-FU affected molecular mechanisms of HCC cells*

To understand the underlying molecular mechanisms, we used Western blot analysis to examine how the combination of tramadol with either cisplatin or 5-FU affects cellular processes such as autophagy, growth, metabolism, ER stress, and ferroptosis. We first examined three important autophagic proteins, including p62, Beclin 1, and LC3B. Beclin 1 has a central role in autophagy which is increased during periods of cell stress and extinguished during the cell cycle.[31] In both HepG2 and Hep3B cells, tramadol increased the amounts of p62 and LC3B II proteins and slightly decreased the amount of beclin 1 (Figure 6A and B). Cisplatin and 5-FU both decreased the amounts of p62 and beclin 1 proteins and had no apparent effect on LC3B II protein. The combination of tramadol increased the amounts of p62, beclin 1, and LC3B II proteins compared with HepG2 cells were treated with cisplatin or 5-FU alone, but only increased the amount of LC3B II protein in Hep3B cells. The combinatory effects of p62 and beclin 1 were restored to basal or lower levels compared with the levels of cisplatin or 5-FU alone when cells treated with higher tramadol doses. The amounts of LC3B proteins by the combinations were lower than related dose of tramadol alone in HepG2 cells, no apparent effect in Hep3B cells.

With respect to cell growth and metabolism, co-treatment with tramadol and either cisplatin or 5-FU markedly reduced the expression of fatty acid synthase (FASN), epidermal growth factor receptor (EGFR), and cyclin D1 in both cell lines. As FASN governs lipid metabolism and EGFR mediates proliferative and survival signalling, their concurrent downregulation indicates that the enhanced anticancer activity of these combinations may result from joint disruption of lipid metabolism and EGFR-driven growth pathways in HCC cells. Cyclin D1 is a protein that controls the transition from G1 to S phase in the cell cycle. Tramadol, cisplatin, and 5-FU alone decreased the amounts of EGFR and cyclin D1 proteins in HepG2 and Hep3B cells. Tramadol, cisplatin, and 5-FU alone increased the amounts of p21 and histone H3 proteins in both cells, the only exception was the effect of cisplatin on p21 protein in Hep3B cells. However, this induction of p21 was attenuated in HepG2 cells when combined 1 mg/ml tramadol with cisplatin or 5-FU,

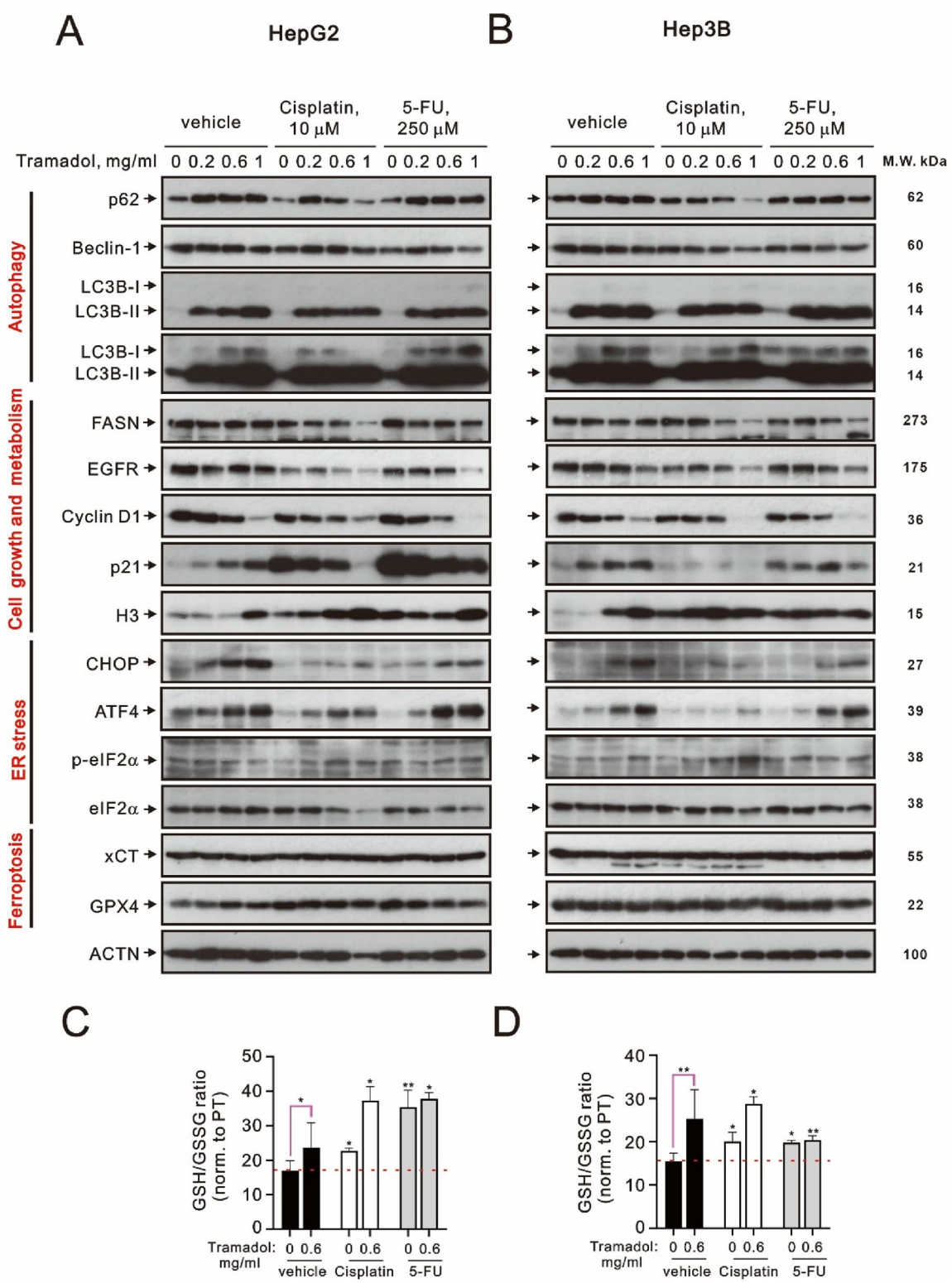



**Figure 6.** The combination of tramadol with cisplatin or 5-FU influenced molecular signalling in HCC cells. (**A**) HepG2 and (**B**) Hep3B cells were treated with tramadol at 0, 0.2, 0.6, and 1 mg/mL combined with 10 μM cisplatin or 250 μM 5-FU for 24 h. The cell lysates, containing 30 μg of total protein, were analysed by Western blotting using antibodies targeting indicated proteins. ACTN was used as a loading control. (**C**) HepG2 and (**D**) Hep3B cells were treated with tramadol at 0 and 0.6 mg/mL combined with 10 μM cisplatin or 250 μM 5-FU for 24 h. The GSH/GSSG ratio was measured using the GSH/GSSG-Glo™ Assay. (**C and D**) The dashed red line is the level for the vehicle control. Bars depict the means ± SDs of three independent experiments. *$p < 0.05$; **$p < 0.01$ (Student's t-tests).

and completely suppressed in Hep3B cells when combined with cisplatin. These cell line–specific responses likely reflect differences in p53 status, as HepG2 is p53 wild-type whereas Hep3B is p53-null, suggesting that tramadol regulates p21 through both p53-dependent and p53-independent mechanisms. Elevated H3 levels may indicate both cell cycle perturbation and active chromatin remodelling.

Regarding ER stress, tramadol alone increased CHOP and ATF4 expressions, whereas this effect of CHOP was suppressed when combined with cisplatin or 5-FU in HepG2 and Hep3B cells. Cisplatin or 5-FU had no effect on CHOP and ATF4 expressions. These findings imply that cisplatin and 5-FU may counteract tramadol-induced ER stress signalling, shifting the stress response away from CHOP-driven apoptosis towards alternative cell death pathways. In addition, tramadol, cisplatin, and 5-FU had no apparent effect on p-eIF2α and eIF2α in both cells. However, the combination of tramadol with cisplatin or 5-FU decreased the amounts of eIF2α proteins in both cells, but the combination of tramadol and cisplatin increased the amount of p-eIF2α protein in Hep3B cells. Finally, in ferroptosis-related signalling, tramadol, cisplatin, and 5-FU induced glutathione peroxidase 4 (GPX4) protein expression in HepG2 cells. Tramadol suppressed these effects on GPX4 proteins by complexed with cisplatin or 5-FU in HepG2 cells. In Hep3B cells, GPX4 expression remained unchanged across all conditions, highlighting a cell type–dependent regulation of ferroptosis by tramadol.

Given that GPX4 activity is critically dependent on glutathione (GSH),[32] we next examined intracellular GSH/GSSG levels to assess redox balance and susceptibility to ferroptosis. Treatment with tramadol, cisplatin, or 5-FU alone resulted in an increased GSH/GSSG ratio in both cell lines, indicating an enhanced antioxidant response (Figure 6C and D). Notably, the combination of tramadol and cisplatin further elevated the GSH/GSSG ratio, suggesting a heightened compensatory defense mechanism. In contrast, the combination of tramadol with 5-FU did not lead to an increase in the GSH/GSSG ratio induced by 5-FU in either HepG2 or Hep3B cells.

## Discussion

In this study, we conducted a systematic investigation into the anti-proliferative, pro-apoptotic, and autophagy-inducing effects of tramadol across three HCC cell lines. Our findings demonstrate that tramadol significantly inhibits cell proliferation in a dose-dependent manner, leading to a reduction in the S-phase and an accumulation of cells in the subG1 phase, alongside mitochondrial depolarisation in HepG2, Hep3B, and Huh7 cells. Focusing specifically on HepG2 and Hep3B cells, we observed that tramadol induces apoptosis, as evidenced by an increase in late apoptosis/necrosis, upregulation of ATF4 and CHOP, and cleavage of PARP and Caspase-3. Furthermore, tramadol significantly enhances the percentage of autophagy, indicated by an accumulation of LC3B-II and modulation of p62 levels. Notably, tramadol also synergistically increased the cytotoxic effects of cisplatin and 5-FU, suggesting a pronounced dose-sparing effect. In summary, our findings reveal that tramadol exerts potent anti-tumour effects in human HCC cells by inhibiting proliferation, inducing apoptosis and autophagy, depolarising mitochondrial membrane potential, and enhancing chemosensitivity. In this study, tramadol was identified as a potential chemosensitizer for HCC. In a translational context, its dual functionality providing both analgesic relief and enhancing chemotherapy effectiveness offers potential benefits for HCC patients.

HCC frequently exhibits mutations in the tumour suppressor protein p53, leading to a loss of its canonical tumour-suppressive functions. In some instances, these mutations can result in gain-of-function activities that promote cell proliferation, tumour progression, and drug resistance.[33] As a result, mutant p53 has become a critical target for the development of anticancer therapies aimed at HCC. p53 acts as a transcription factor that regulates DNA damage repair, cell cycle arrest, and apoptosis, thereby controlling cell proliferation and maintaining genomic stability.[34] It is estimated that p53 is mutated in approximately half of all human cancers, often resulting in the loss of tumour-suppressive activity or, in certain gain-of-function mutations, the acquisition of oncogenic properties.[35] Within the context of HCC cell lines, Hep3B cells lack p53 due to a homozygous deletion, HepG2 expresses wild-type p53, and Huh7 carries a mutant codon with notable p53 overexpression. Remarkably, tramadol inhibited cellular proliferation and induced mitochondrial depolarisation across all three HCC cell lines, regardless of their p53 status. These findings indicate that the anti-cancer effects of tramadol are primarily independent of p53, highlighting its potential as a therapeutic option for

HCC tumours with p53 mutations. Our results demonstrate that tramadol stimulates the expression of the p21 protein and induces apoptosis while decreasing Bax protein levels in both HepG2 cells, which have wild-type p53, and Hep3B cells, which lack p53. This suggests that tramadol can modulate p21 through both p53-dependent and p53-independent pathways. The genetic status of p53, along with a paradoxical immune response, can promote the malignant growth of HCC tumours.[36] Tramadol has been shown to suppress the growth of orthotopic liver tumours by promoting the polarisation of M1 macrophages in the tumour microenvironment.[37] In addition to repurposing existing drugs, traditional Chinese medicines that target multiple pathways associated with chronic inflammation present promising options for developing therapies for HCC, such as *Artemisia rupestris* L.[38]

The strategic selection of cell death inducers or the combined modulation of multiple death pathways presents a promising approach to overcoming drug resistance and effectively targeting metastatic cancer cells.[39,40] Currently, chemotherapy is not the first-line treatment for HCC patients, but it can be used in combination with immunotherapy, targeted therapy, or other chemotherapeutic agents.[4,41,42] In our study, tramadol exhibited a notable synergistic effect when combined with cisplatin and 5-FU, significantly lowering the IC50 values of these chemotherapeutic agents. In conjunction with additional related clinical trials, the role of tramadol as a chemosensitizer suggests the possibility of reducing the necessary doses of cisplatin and 5-FU. This approach could minimise their associated toxicities while preserving or even enhancing therapeutic efficacy. The role of tramadol as a chemotherapy sensitiser has been established in human breast and cervical cancer cells.[22,43] In the context of HCC, tramadol also acts as a modulator of M1 macrophages.[37] Importantly, tramadol may provide dual benefits in HCC treatment by offering effective analgesia while simultaneously enhancing the anti-tumour activity of chemotherapeutic agents. This dose-sparing, multi-faceted strategy could substantially improve the quality of life for patients who frequently experience both cancer-related pain and chemotherapy-induced side effects. Repurposing strategies have identified several candidate drugs, including metformin, disulphiram, and atorvastatin, as potential sensitisers for the treatment of HCC.[44–46]

Interestingly, this combinatory effect did not affect the tramadol-induced increase in LC3B-II levels. Our findings demonstrate that tramadol simultaneously induced apoptosis and autophagy in HCC cells, raising important questions about the interplay between these two processes. However, it remains uncertain whether, in our system, autophagy primarily promotes tramadol-induced apoptosis or represents a protective response by the cells attempting to resist tramadol's cytotoxic effects. This distinction is crucial for guiding future research. Numerous autophagy-related molecules and signalling pathways are intricately linked to apoptotic pathways, and the crosstalk between these processes can significantly influence cell fate. On one hand, autophagy can enhance the survival of cancer cells under stress, thereby attenuating apoptosis and necroptosis.[47] Conversely, excessive or dysregulated autophagy can inhibit metastasis by limiting tumour necrosis and subsequent immune cell infiltration, while overactivation may induce the death of metastatic cells.[48] The inconsistency observed among the decrease in Bax, mitochondrial depolarisation, and caspase/PARP activation in our data highlights the complex interactions between various forms of cell death and cancer progression. These findings emphasise the intricate relationship that exists within these pathways.

Oxidative stress occurs when there is an imbalance between the production of ROS and the body's antioxidant capacity.[49] Our data revealed that tramadol, cisplatin, and 5-FU elevated the GSH/GSSG ratio in HepG2 and Hep3B cells. Notably, tramadol enhanced the GSH/GSSG ratio of cisplatin, but not of 5-FU, in both cell lines. These discrepancies could arise from limited access of ROS analytical agents to their targets, as well as differences in subcellular localisation. As such, these gaps and the underlying mechanisms warrant further exploration. The nuclear factor erythroid 2-related factor 2 (Nrf2)/Kelch-like ECH-associated protein 1 (Keap1) pathway is a well-known signalling route that plays a crucial role in combating oxidative stress and providing cellular protection.[50] In vertebrates, p62 is known to sense the saturation of ROS-buffering systems, and this redox sensitivity is essential for promoting autophagy, thereby ensuring cell survival under oxidative stress conditions.[30] Therefore, p62 may play a role in the anti-oxidative capacity of tramadol when used in conjunction with cisplatin, but not with 5-FU. The specific regulatory mechanisms involved warrant further investigation. Additionally, further genetic and pharmacological studies are necessary to elucidate the causal ATF4/CHOP pathway induced by tramadol.

The therapeutic blood levels of tramadol in adults typically range from 0.1 to 0.3 μg/mL.[51] However, the concentrations of tramadol used in our study (0.2–1 mg/mL) to achieve its anti-cancer effects exceed those typically used for clinical analgesia, representing a significant limitation. This approach is informed by the

understanding that *in vitro* systems often require higher extracellular drug levels to induce measurable cellular responses, such as cytotoxicity, compared to the concentrations associated with adverse effects observed *in vivo*.[52] *O*-desmethyltramadol, the primary active metabolite of tramadol, exhibits similar cytotoxicity against breast cancer cells even at significantly lower concentrations than those of tramadol.[53] Importantly, neither tramadol nor *O*-desmethyltramadol demonstrated cytotoxic effects through μ-opioid receptor signalling in breast cancer cells. Additionally, transcriptomic analyses revealed that tramadol and *O*-desmethyltramadol differentially modulated gene expression profiles across various breast cancer subtypes. The mechanisms underlying these effects suggest that tramadol induces paraptosis-like cell death via HIF-1α and ATF4-dependent pathways.[28] Considering the differences in cell death mechanisms between breast cancer and HCC, future research is essential to identify target receptors and investigate specific signalling networks that elucidate the molecular mechanisms behind the enhanced anti-tumour efficacy in HCC. Furthermore, our repurposing strategy conducted in an *in vitro* cultured system highlights the necessity for additional pharmacokinetic and pharmacodynamic studies to assess the potential impact of tramadol concentration and accumulation in oncology settings, particularly for patients undergoing prolonged tramadol therapy.

## Conclusion

In this study, we investigated the anti-proliferative, pro-apoptotic, and autophagy-inducing effects of tramadol in three HCC cell lines: HepG2, Hep3B, and Huh7. Our results indicate that tramadol significantly inhibits cell proliferation in a dose-dependent manner, leading to a reduction in the S-phase and an accumulation of cells in the subG1 phase alongside mitochondrial depolarisation. In HepG2 and Hep3B cells, tramadol induced apoptosis, evidenced by increased late apoptosis/necrosis, upregulation of ATF4 and CHOP, and cleavage of PARP and Caspase-3. Additionally, tramadol enhanced the percentage of autophagy, as demonstrated by the accumulation of LC3B-II and modulation of p62. Notably, tramadol increased the cytotoxicity of cisplatin and 5-FU with combination indices below 1 in HepG2 and Hep3B cells. Finally, additional pharmacokinetic and pharmacodynamic studies are necessary to evaluate the potential impact of tramadol concentration and accumulation in oncology settings for liver cancer patients.

## Author contributions

CRediT: **Hsiu-Lung Fan**: Conceptualization, Formal analysis, Investigation, Methodology, Supervision, Writing – original draft; **Shu-Ting Liu**: Data curation, Formal analysis, Validation; **Zih-Syuan Wu**: Data curation; **Yi-Hsuan Huang**: Conceptualization, Funding acquisition, Methodology, Supervision; **Shih-Ming Huang**: Conceptualization, Funding acquisition, Methodology, Validation; **Teng-Wei Chen**: Conceptualization, Funding acquisition, Investigation, Supervision, Writing – original draft, Writing – review & editing; **Zhi-Fu Wu**: Conceptualization, Formal analysis, Funding acquisition, Investigation, Supervision, Writing – original draft, Writing – review & editing.

## Disclosure statement

No potential conflict of interest was reported by the author(s).

## Funding

This work was supported by grants from the Tri-Service General Hospital [TSGH-E–115216 to T-W Chen], the Ministry of National Defense-Medical Affairs Bureau [MND-MAB–112–069 to S-M Huang], the Teh-Tzer Study Group for Human Medical Research Foundation [B1141022 to S-M Huang], and the National Science and Technology Council [NSTC 112–2314-B016-067 and NSTC 115–2314-B-016–070 to Y-H Huang and NSTC 115–2314-B-650–006 to Z-F Wu], Taiwan, Republic of China.

## Data availability statement

The data generated during the current study is available from the corresponding author upon reasonable request.

## References


1. Mauro E, de Castro T, Zeitlhoefler M, Sung MW, Villanueva A, Mazzaferro V, Llovet JM. Hepatocellular Carcinoma: Epidemiology, diagnosis and treatment. JHEP Rep. 2025;7(12):101571.
2. Tan EY, Danpanichkul P, Yong JN, Yu Z, Tan DJH, Lim WH, Koh B, Lim RYZ, Tham EKJ, Mitra K, et al. Liver cancer in 2021: Global Burden of Disease study. J Hepatol. 2025;82(5):851–860.
3. Oh JH, Jun DW. The latest global burden of liver cancer: a past and present threat. Clin Mol Hepatol. 2023;29(2):355–357.
4. Llovet JM, Kelley RK, Villanueva A, Singal AG, Pikarsky E, Roayaie S, Lencioni R, Koike K, Zucman-Rossi J, Finn RS. Hepatocellular carcinoma. Nat Rev Dis Primers. 2021;7(1):6.
5. Vogel A, Meyer T, Sapisochin G, Salem R, Saborowski A. Hepatocellular carcinoma. Lancet. 2022;400(10360):1345–1362.,
6. Sutanto H, Adytia GJ, Elisa E, Maimunah U. Advances in transarterial chemoembolization for hepatocellular carcinoma: Integration with systemic therapies and emerging treatment strategies. Cancer Pathog Ther. 2026;4(1):1–13.
7. Sethy C, Kundu CN. 5-Fluorouracil (5-FU) resistance and the new strategy to enhance the sensitivity against cancer: Implication of DNA repair inhibition. Biomed Pharmacother. 2021;137:111285.
8. Ghosh S. Cisplatin: The first metal based anticancer drug. Bioorg Chem. 2019;88:102925.
9. Karasawa T, Steyger PS. An integrated view of cisplatin-induced nephrotoxicity and ototoxicity. Toxicol Lett. 2015;237(3):219–227.
10. Zhu L, Li J, Wang ZQ, Gu YJ, Li GN, Wang WJ, Pen GB, Li Q, Wu MD, Liu HR, et al. Treatment of moderate-to-severe pain in hepatocellular carcinoma with transcutaneous electrical acupoint stimulation: a randomized controlled trial. J Pain Res. 2024;17:1583–1594.
11. Scroope CA, Singleton Z, Hollmann MW, Parat MO. Opioid receptor-mediated and non-opioid receptor-mediated roles of opioids in tumour growth and metastasis. Front Oncol. 2021;11:792290.
12. Chen DT, Pan JH, Chen YH, Xing W, Yan Y, Yuan YF, Zeng WA. The mu-opioid receptor is a molecular marker for poor prognosis in hepatocellular carcinoma and represents a potential therapeutic target. Br J Anaesth. 2019;122(6):e157–e167.
13. Zhang JJ, Song CG, Dai JM, Zhang XQ, Lin P, Li L, Yang XM, Chen ZN. Inhibition of mu-opioid receptor suppresses proliferation of hepatocellular carcinoma cells via CD147-p53-MAPK cascade signaling pathway. Am J Transl Res. 2021;13(5):3967–3986.
14. Li Y, Li G, Tao T, Kang X, Liu C, Zhang X, Wang C, Li C, Guo X. The mu-opioid receptor (MOR) promotes tumor initiation in hepatocellular carcinoma. Cancer Lett. 2019;453:1–9.
15. Wei YC, Zhang B, Li X, Liu XM, Zhang J, Lei B, Li B, Zhai R, Chen Q, Li Y. Upregulation and activation of delta-opioid receptors promotes the progression of human breast cancer. Oncol Rep. 2016;36(5):2579–2586.
16. Chen D, Chen Y, Yan Y, Pan J, Xing W, Li Q, Zeng W. Down-regulation of the tumour suppressor kappa-opioid receptor predicts poor prognosis in hepatocellular carcinoma patients. BMC Cancer. 2017;17(1):553.
17. Kim JY, Ahn HJ, Kim JK, Kim J, Lee SH, Chae HB. Morphine suppresses lung cancer cell proliferation through the interaction with opioid growth factor receptor: an in vitro and human lung tissue study. Anesth Analg. 2016;123(6):1429–1436.
18. Subedi M, Bajaj S, Kumar MS, Yc M. An overview of tramadol and its usage in pain management and future perspective. Biomed Pharmacother. 2019;111:443–451.
19. Kim MH, Oh JE, Park S, Kim JH, Lee KY, Bai SJ, Song H, Hwang HJ, Kim DW, Yoo YC. Tramadol use is associated with enhanced postoperative outcomes in breast cancer patients: a retrospective clinical study with in vitro confirmation. Br J Anaesth. 2019;123(6):865–876.
20. Kim MH, Lee J-R, Kim K-J, Jun JH, Hwang HJ, Lee W, Nam SH, Oh JE, Yoo YC. Identification for antitumor effects of tramadol in a xenograft mouse model using orthotopic breast cancer cells. Sci Rep. 2021;11(1):22113.
21. Liu L-C, Wu Z-S, Chen J-L, Wu Z-F, Lai H-C, Huang Y-H. Mitochondrial dysfunction involved in the cytotoxicity of tramadol in human endometrial carcinoma cells. Int J Mol Sci. 2022;24(1):99.
22. Huang YH, Sue SH, Wu ZS, Huang SM, Lee SY, Wu ZF. Antitumorigenic effect of tramadol and synergistic effect with doxorubicin in human breast cancer cells. Front Oncol. 2022;12:811716.
23. Chou TC. Theoretical basis, experimental design, and computerized simulation of synergism and antagonism in drug combination studies. Pharmacol Rev. 2006;58(3):621–681.
24. Zorova LD, Popkov VA, Plotnikov EY, Silachev DN, Pevzner IB, Jankauskas SS, Babenko VA, Zorov SD, Balakireva AV, Juhaszova M, et al. Mitochondrial membrane potential. Anal Biochem. 2018;552:50–59.
25. Qiu GH, Xie X, Xu F, Shi X, Wang Y, Deng L. Distinctive pharmacological differences between liver cancer cell lines HepG2 and Hep3B. Cytotechnology. 2015;67(1):1–12.
26. Han J, Back SH, Hur J, Lin YH, Gildersleeve R, Shan J, Yuan CL, Krokowski D, Wang S, Hatzoglou M, et al. ER-stress-induced transcriptional regulation increases protein synthesis leading to cell death. Nat Cell Biol. 2013;15(5):481–490.

27. Delbrel E, Soumare A, Naguez A, Label R, Bernard O, Bruhat A, Fafournoux P, Tremblais G, Marchant D, Gille T, et al. HIF-1alpha triggers ER stress and CHOP-mediated apoptosis in alveolar epithelial cells, a key event in pulmonary fibrosis. Sci Rep. 2018;8(1):17939.
28. Wu ZS, Huang SM, Huang YH. Tramadol induced hypoxia signaling and paraptosis-like cell death in breast cancer cells via HIF-1alpha and ATF4 dependent pathways. Redox Rep. 2026;31(1):2588866.
29. Chipuk JE, Kuwana T, Bouchier-Hayes L, Droin NM, Newmeyer DD, Schuler M, Green DR. Direct activation of Bax by p53 mediates mitochondrial membrane permeabilization and apoptosis. Science. 2004;303(5660): 1010–1014.
30. Carroll B, Otten EG, Manni D, Stefanatos R, Menzies FM, Smith GR, Jurk D, Kenneth N, Wilkinson S, Passos JF, et al. Oxidation of SQSTM1/p62 mediates the link between redox state and protein homeostasis. Nat Commun. 2018;9(1):256.
31. Kang R, Zeh HJ, Lotze MT, Tang D. The Beclin 1 network regulates autophagy and apoptosis. Cell Death Differ. 2011;18(4):571–580.
32. Yan HF, Zou T, Tuo QZ, Xu S, Li H, Belaidi AA, Lei P. Ferroptosis: mechanisms and links with diseases. Signal Transduct Target Ther. 2021;6(1):49.
33. Azer SA. MDM2-p53 Interactions in Human Hepatocellular Carcinoma: What Is the Role of Nutlins and New Therapeutic Options? J Clin Med. 2018;7(4):64.
34. Wang H, Guo M, Wei H, Chen Y. Targeting p53 pathways: mechanisms, structures and advances in therapy. Signal Transduct Target Ther. 2023;8(1):92.
35. Shetzer Y, Molchadsky A, Rotter V. Oncogenic mutant p53 gain of function nourishes the vicious cycle of tumor development and cancer stem-cell formation. Cold Spring Harb Perspect Med. 2016;6(10):a026203. a026203.
36. Zhao J, Li Y, Zhu J, Li H, Jin X. Ubiquitination in hepatocellular carcinoma immunity. J Transl Med. 2025; 23(1):574.
37. Wang L, Guo W, Guan H, Yan N, Cai X, Zhu L. Tramadol suppresses growth of orthotopic liver tumors via promoting M1 macrophage polarization in the tumor microenvironment. Naunyn Schmiedebergs Arch Pharmacol. 2024;397(6):4205–4218.
38. Zhang S, Li J, Ding M, Khan GJ, Abuduaini A, Chang Y, Mao Y, Hu H, Zhai K. Dual targeting by Artemisia rupestris L. disrupting TLR4/NF-kappaB signaling and macrophage driven immune evasion in hepatocellular carcinoma. J Ethnopharmacol. 2026;358:121028.
39. Bhat GR, Sethi I, Sadida HQ, Rah B, Mir R, Algehainy N, Albalawi IA, Masoodi T, Subbaraj GK, Jamal F, et al. Cancer cell plasticity: from cellular, molecular, and genetic mechanisms to tumor heterogeneity and drug resistance. Cancer Metastasis Rev. 2024;43(1):197–228.
40. Liu B, Zhou H, Tan L, Siu KTH, Guan XY. Exploring treatment options in cancer: Tumor treatment strategies. Signal Transduct Target Ther. 2024;9(1):175.
41. Llovet JM, Castet F, Heikenwalder M, Maini MK, Mazzaferro V, Pinato DJ, Pikarsky E, Zhu AX, Finn RS. Immunotherapies for hepatocellular carcinoma. Nat Rev Clin Oncol. 2022;19(3):151–172.
42. Llovet JM, Montal R, Sia D, Finn RS. Molecular therapies and precision medicine for hepatocellular carcinoma. Nat Rev Clin Oncol. 2018;15(10):599–616.
43. He B, Tong X, Wang L, Wang Q, Ye H, Liu B, Hong X, Tao L, Harris AL. Tramadol and flurbiprofen depress the cytotoxicity of cisplatin via their effects on gap junctions. Clin Cancer Res. 2009;15(18):5803–5810.
44. Xiong Y, Lu QJ, Zhao J, Wu GY. Metformin inhibits growth of hepatocellular carcinoma cells by inducing apoptosis via mitochondrion-mediated pathway. Asian Pac J Cancer Prev. 2012;13(7):3275–3279.
45. Lin H, Sun F, Li T, Zhang Y, Guo X, Li M, Liang M, Zhou X, Fang Z. Disulfiram enhances chemotherapeutic effects of doxorubicin liposomes against human hepatocellular carcinoma via activating ROS-induced cell stress response pathways. Cancer Chemother Pharmacol. 2022;90(6):455–465.
46. Wang ST, Huang SW, Liu KT, Lee TY, Shieh JJ, Wu CY. Atorvastatin-induced senescence of hepatocellular carcinoma is mediated by downregulation of hTERT through the suppression of the IL-6/STAT3 pathway. Cell Death Discov. 2020;6:17.
47. Su Z, Yang Z, Xu Y, Chen Y, Yu Q. Apoptosis, autophagy, necroptosis, and cancer metastasis. Mol Cancer. 2015;14(1):48.
48. Jiang G-M, Tan Y, Wang H, Peng L, Chen H-T, Meng X-J, Li L-L, Liu Y, Li W-F, Shan H. The relationship between autophagy and the immune system and its applications for tumor immunotherapy. Mol Cancer. 2019;18(1):17.
49. Sies H, Berndt C, Jones DP. Oxidative stress. Annu Rev Biochem. 2017;86:715–748.
50. Ahmed SM, Luo L, Namani A, Wang XJ, Tang X. Nrf2 signaling pathway: Pivotal roles in inflammation. Biochim Biophys Acta Mol Basis Dis. 2017;1863(2):585–597.
51. Manouchehri A, Nekoukar Z, Malakian A, Zakariaei Z. Tramadol poisoning and its management and complications: a scoping review. Ann Med Surg. 2023;85(8):3982–3989.
52. Albrecht W. Which concentrations are optimal for in vitro testing? Excli j. 2020;19:1172–1173.
53. Wu ZS, Huang YH, Huang SM. O-Desmethyltramadol enhanced anti-cancer efficacy over tramadol through non-mu-opioid receptor and differential cellular contexts of human breast cancer cells. Int J Mol Sci. 2025;26(9):4139.